Biophysical Journal, Volume *121*

Supplemental information

A vesicle microrheometer for high-throughput viscosity measurements of lipid and polymer membranes

Hammad A. Faizi, Rumiana Dimova, and Petia M. Vlahovska

Supplementary Material: A vesicle microrheometer for high-throughput viscosity measurements of lipid and polymer membranes

Hammad A. Faizi,[1] Rumiana Dimova,[2] and Petia M. Vlahovska[3]

[1] *Department of Mechanical Engineering, Northwestern University, Evanston, IL 60208, USA*
[2] *Department of Theory and Biosystems, Max Planck Institute of Colloids and Interfaces, Science Park Golm, 14424 Potsdam, Germany*
[3] *Department of Engineering Sciences and Applied Mathematics, Northwestern University, Evanston, IL, 60208, USA, email: petia.vlahovska@northwestern.edu*

1. SHAPE EVOLUTION OF QUASI-SPHERICAL VESICLE IN A UNIFORM ELECTRIC FIELD

A. Summary of the theoretical model

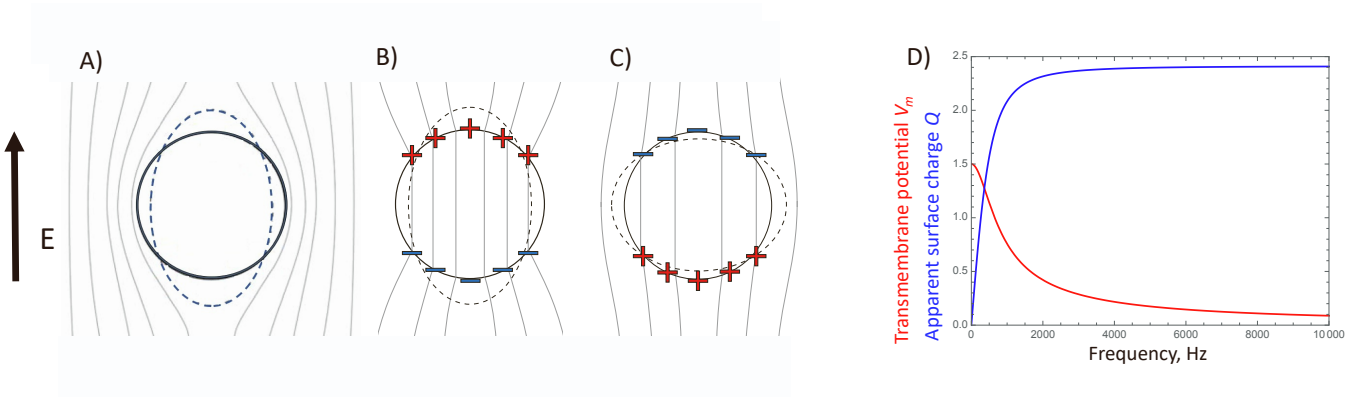

Fig. S 1: (A)-(C) Physical mechanisms of the frequency-dependent membrane polarization and vesicle dipole in an applied uniform AC field. The lines correspond to constant electric field. Upon application of an external electric field, charges accumulate on the two sides of the membrane setting up a potential difference, i.e., the membrane acts as a capacitor. (A) At low frequencies, $\omega \ll \omega_c$, the membrane capacitor is fully charged, the induced charge density on the two membrane surfaces is the same but of opposite sign. (B) and (C) At intermediate frequencies, $\omega > \omega_c$, it is short-circuited and there is charge imbalance between the inner and outer membrane surfaces $Q = \varepsilon E_0 Q_0 \cos\theta$. (B) If the enclosed solution is more conducting than the suspending medium, $\Lambda > 1$, vesicle is pulled into an prolate ellipsoid. (C) The polarization is reversed in the opposite case $\Lambda < 1$ and the vesicle deforms into an oblate ellipsoid. (D) Variation with frequency of the transmembrane potential (red) and apparent charge at the pole (blue).

Let us consider a vesicle made of a charge-free lipid bilayer membrane with bending rigidity κ, tension $\sigma_{\rm eq}$, capacitance $C_{\rm m}$. The vesicle is suspended in a solution with conductivity $\lambda_{\rm ex}$ and permittivity $\varepsilon_{\rm ex}$, and filled with a different solution characterized by $\lambda_{\rm in}$ and $\varepsilon_{\rm in}$.

An axisymmetric stress, such as generated by uniform electric field or extensional flow, deforms the vesicle into a spheroid with symmetry axis aligned with the extensional axis. The spheroid aspect ratio is $\nu = a/b$, where a is the length of the symmetry axis and b is the length of the axis perpendicular to the symmetry axis. For small deformations, $\nu \lesssim 1.3$, the shape is well approximated by

$$r_s(\theta) = R\left(1 + \frac{s}{2}\left(1 + 3\cos 2\theta\right)\right), \tag{S1}$$

where r_s is the position of the surface, R is the initial radius of the vesicle, s is the deformation parameter, and θ is the angle with the applied field direction; $\theta = 0$ and $\pi/2$ correspond to the pole and the equator, respectively. The ellipsoid aspect ratio is related to the deformation parameter by $\nu = (1+s)/(1-2s)$.

The theory developed by *Vlahovska et al.* [1–4] predicts that the deformation parameter evolution is given by the balance of imposed and membrane stresses

$$\dot{s} = \frac{1}{32 + 23\chi + 16\chi_m}\left(\frac{\varepsilon_{\rm ex} E_0^2 p^{\rm el}}{\eta} - 24 s(6\kappa + \sigma(s)R^2)\frac{1}{\eta R^3}\right) \tag{S2}$$

For small deformations, $s \ll 1$, $\nu \sim 1 + 3s$ and the above equation yields Eq. 1 in the main text.

The AC field, $E(t) = E_0 \sin(\omega t)$, generates an electric stress which has two components, a steady one $p^{\rm el}$ and an oscillatory one with frequency twice the applied one

$$p = p^{\rm el} + p^c_\omega \cos(2\omega t) + p^s_\omega \sin(2\omega t)$$

In the experiments typically $\bar{\omega} \gg 1$ and the oscillatory component only drives very small oscillations about the deformation induced by the steady stress component.

The steady electric stress is given by

$$p^{\rm el} = 2(1 - P^r_{\rm ex}) + \frac{1}{2} P^2_{\rm ex} - 2S P^2_{\rm in} \tag{S3}$$

and the amplitudes of the unsteady stress are

$$\begin{aligned} p^c_\omega &= \frac{1}{2}\left(4(1 - P^r_{\rm ex}) - \left(P^i_{\rm ex}\right)^2 + \left(P^r_{\rm ex}\right)^2 - 4S\left(\left(P^i_{\rm in}\right)^2 + \left(P^r_{\rm in}\right)^2\right)\right) \\ p^s_\omega &= 2P^i_{\rm ex} - P^i_{\rm ex} P^r_{\rm ex} + 4S P^i_{\rm in} P^r_{\rm in} \end{aligned} \tag{S4}$$

where

$$\begin{aligned} P_{\rm ex} =& \frac{K_{\rm ex} + K_{\rm in}(V_m - 1)}{K_{\rm in} + 2K_{\rm ex}}, \quad P_{\rm in} = \frac{K_{\rm ex}(3 - 2V_m)}{K_{\rm in} + 2K_{\rm ex}}, \\ V_m =& \frac{3K_{\rm in}K_{\rm ex}}{2K_{\rm in}K_{\rm ex} + {\rm i}C_{\rm m}\left(K_{\rm in} + 2K_{\rm ex}\right)\bar{\omega}} \end{aligned} \tag{S5}$$

Here $\bar{\omega} = \omega \varepsilon_{\rm ex}/\lambda_{\rm ex}$ and $\bar{C}_{\rm m} = C_{\rm m} R/\varepsilon_{\rm ex}$ are the dimensionless frequency and membrane capacitance. $K_{\rm in} = 1 + {\rm i}\bar{\omega}$ and $K_{\rm ex} = \Lambda + {\rm i}\bar{\omega} S$ are the dimensionless complex permittivities. $S = \varepsilon_{\rm in}/\varepsilon_{\rm ex}$ and $\Lambda = \lambda_{\rm in}/\lambda_{\rm ex}$ are the ratios of permittivities and conductivities of the fluids interior and exterior to the vesicle. P^r and P^i denote the real and imaginary part of P, and $P^2 = PP^*$, where the superscript * denotes complex conjugate. The electric stress in DC field is obtained by setting $\bar{\omega} = 0$ and the electric field amplitude to $E_0\sqrt{2}$.

Typically, both the inner and outer fluids are aqueous solutions with similar permittivities, $\varepsilon_{\rm in} \approx \varepsilon_{\rm ex} = \varepsilon$, hence S can be set to 1. In this case Eq. S3 reduces to

$$p^{\rm el} = \frac{9\left[\bar{\omega}^2\left(\bar{C}^2_{\rm m}(\Lambda+2)^2(\Lambda-1)(\Lambda+3) + 2\bar{C}_{\rm m}\Lambda\left(\Lambda^2+\Lambda-2\right) + 9\Lambda^2\right) + \Lambda^2(\Lambda+2)^2\right]}{2\left((\Lambda+2)^2 + 9\bar{\omega}^2\right)\left(\bar{C}^2_{\rm m}(\Lambda+2)^2\bar{\omega}^2 + 4\Lambda^2\right)}, \tag{S6}$$

where $\bar{\sigma} = \sigma R^2/\kappa$. At low frequencies, $\bar{\omega} \to 0$, the membrane capacitor is fully charged, and $p^{\rm el} = 9/16$ and we obtain Equation 1 in the main text.

The imbalance between the induced charge of the two membrane surfaces is $Q = \varepsilon E_0 Q_0 \cos\theta$, where the maximum charge is

$$Q_0 = \frac{3\bar{\omega} C_m (\Lambda - 1)(\Lambda + 2)}{\left[\left((2+\Lambda)^2 + 9\bar{\omega}^2\right)\left(4\Lambda^2 + C^2_m\bar{\omega}^2(2+\Lambda)^2\right)\right]^{1/2}} \tag{S7}$$

At low frequencies, $\bar{\omega} \to 0$ the charge imbalance vanishes.

B. Linear approximation of the evolution equation

The tension in Eq. S2 is of entropic origin and depends nonlinearly on deformation [5]. For a quasi-spherical vesicle

$$\sigma = \sigma_0 \exp\left(\frac{8\pi\kappa}{k_B T}\alpha\right) \tag{S8}$$

where $\alpha = (A - A_0)/A_0$ is the area strain (the difference between the area of the deformed vesicle A and a sphere with the same volume A_0). For small deformations, $\alpha = 8s^2/5$ [6]. For aspect ratios smaller than 1.1, such as during the early deformation, the area strain is very small and tension remains close to the equilibrium tension σ_0. Assuming constant tension, Eq. 2 in the main text can be integrated to yield

$$\nu(t) = 1 + \frac{pR}{24\sigma}\left(1 - \exp\left(-\frac{24\sigma}{\eta R\left(55 + 16\chi_m\right)}t\right)\right) \tag{S9}$$

If

$$\frac{24\sigma t}{\eta R\,(55+16\chi_m)} \ll 1$$

the exponent is expanded in Taylor series to yield the linear evolution, Eq. 2 in the main text.

The time limit for the linear approximation can be estimated by comparing the linear and quadratic terms in the Taylor series of the exponential term in Eq. S9. The Taylor series of the exponential function is

$$\exp(-ct) = 1 - ct + \frac{(ct)^2}{2} + h.o.t. \quad \text{where for Eq. S9} \quad c = \frac{24\sigma}{\eta R\,(55+16\chi_m)}$$

It shows that the quadratic correction becomes comparable to the linear term when

$$ct = \frac{(ct)^2}{2} \Longrightarrow t = \frac{2}{c}$$

which gives the estimate for the time up to which the linear approximation is reasonable

$$\frac{t}{t_\mathrm{d}} = \frac{\varepsilon E_0^2 R\,(55+16\chi_m)}{12\sigma}$$

Considering typical parameters, $\sigma_0 = 10^{-8}$ N/m, $\kappa = 25k_BT$, $E_0 = 10$ kV/m, $R = 10\,\mu$m gives $\varepsilon E_0^2 R/\sigma \sim 1$, where σ is evaluated from Eq. S8 using aspect ratio $\nu = 1.2$. Thus the linear regime extends to $t/t_\mathrm{d} \sim 1$ if $\chi_m \sim 1$. Higher membrane viscosity lengthens the linear deformation regime, e.g., if $\chi_m \sim 10$, as in polymersomes made of PBd_{22}-*b*-PEO_{14}, the cut-off time becomes $t/t_\mathrm{d} \sim 15$, see Fig. Fig. S2a

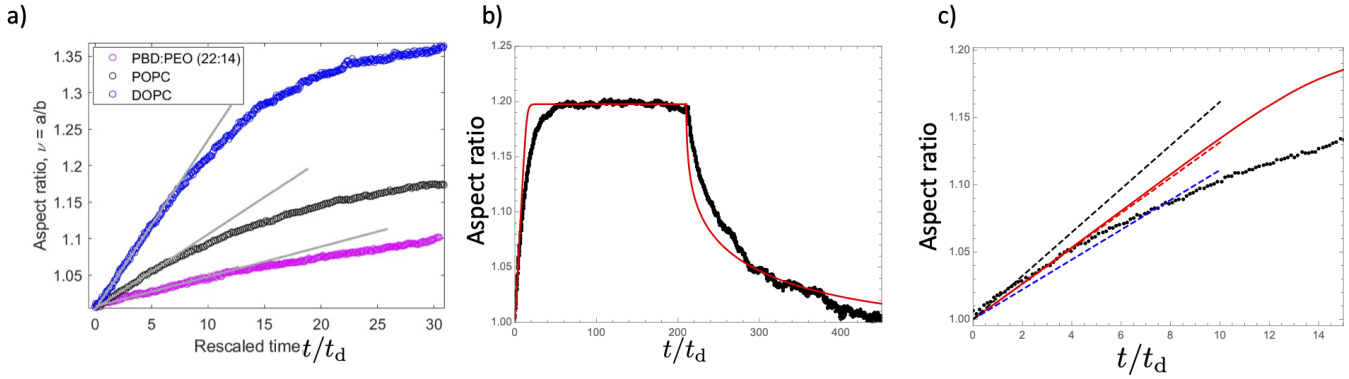

Fig. S 2: a) Vesicle deformation as a function of the dimensionless time t/t_d. (b) Fit of the deformation/relaxation curve of the POPC vesicle shown on Figure 1 in the main text. Solid line is computed from Eq. S2 with parameters $\chi_m = 10$ while field is on, $\chi_m = 0$ after the field is turned off, bending rigidity $\kappa = 25k_BT$ and initial tension $\sigma_0 = 3\times10^{-8}$ N/m. (c) Zoom into the initial deformation showing the initial slopes $\chi_m = 10$ (red) and $\pm25\%$ deviation, $\chi_m = 12.5$ (black) and $\chi_m = 7.5$ (blue).

In principle, Eq. S2 could be used to fit he whole deformation and relaxation curve (note that Eq. S9 is an approximation derived from Eq. S2 assuming constant tension, which implies very small vesicle deformation, aspect ratio <1.1) If the whole data set were to be used, this would require a nonlinear fit using Eq. S2 (since it can not be analytically integrated to give $\nu(t)$ because tension increases exponentially with area strain, see Eq. S8) with at least two parameters – viscosity and initial tension (if bending rigidity is known). Such fit is challenging. Furthermore, the effect of the deformation in the theory (second term in Eq. S2) is an approximation - it only includes the linear correction for the deviation from a sphere and as a result there is an error introduced by neglecting the higher order terms; this error can become significant as aspect ratio increases. Figure Fig. S2b,c does show that the theory does not match well the vesicle deformation at times where the tension is operational, indicating limitations of the theory that likely arise from a break-down of the small deformation assumption and/or modification of the membrane elastic properties (tension and bending rigidity) by the electric field (for example, there could be an electric field induced contribution to the tension [7, 8])

Thus, the errors arising from the nonlinear fit and the shape approximation are likely to negatively affect the accuracy with which the viscosity is determined. It is really fortuitous that vesicles have the initial linear deformation regime, due to their very low tension, which leads to a large difference between the rate with which electric stresses deform the vesicle,$t_\mathrm{d}^{-1} \sim \eta/\varepsilon E_0^2$, and the rate with which the tension pulls the vesicle back to its equilibrium spherical shape,$t_\sigma^{-1} \sim \eta R/\sigma_0$. The ratio of these two rates $t_\mathrm{d}^{-1}/t_\sigma^{-1} = \sigma/\varepsilon E_0^2 R \gg 1$ indicates that the initial deformation is entirely dominated by the electric stresses (and insensitive to tension).

2. ADDITIONAL DATA

A. Batch reproducibility for homogeneous (DOPC) and mixed membrane compositions (DOPC:DPPC:Chol (1:1:1))

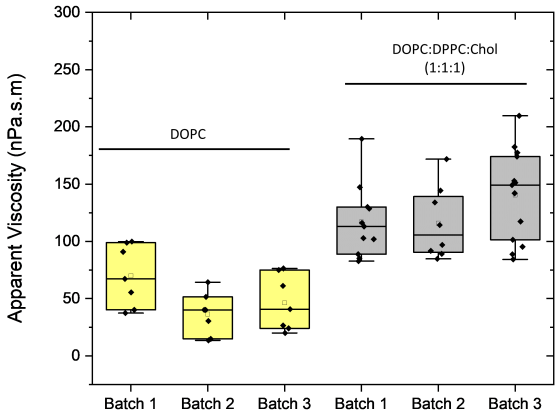

Fig. S 3: Method reproducibility for the same system across different batches: Membrane viscosity for DOPC and DOPC:DPPC:Chol (1:1:1) for three different batches of prepared vesicles. The applied frequency and field strength are 1 kHz and 10 kV/m for respectively. For DOPC:DPPC:Chol (1:1:1), the applied frequency is 2 kHz and and applied field strength is 6 kV/m. The solid symbols show measurements on individual vesicles. The box-plot represents the standardized distribution of data based on five numbers minimum value, first quartile (Q1), median, third quartile (Q3), and maximum value. The open square represents the mean value. The numerical data is summarized in Table S3.

Figure Fig. S3 shows the box plot presentation for apparent membrane viscosity values obtained for the same system across three different batches of vesicles prepared from DOPC and DOPC:DPPC:Chol (1:1:1). The zero charge or frequency membrane viscosity data is given in the main text.

B. Deformation curves of bilayers at different field strength and frequency

Figure Fig. S4A represents deformation curves of POPC vesicles at different field strength (6-10 kV/m) at frequency 1 kHz. In Figure Fig. S4B the data is re-plotted again in rescaled time with t_{d}. The inverse of t_{d} can be expressed as shear rate, $\dot{\gamma}$ which in this case ranges from, $\dot{\gamma}$ ∼10-100 s^{-1}. The collapse of the data on single curve indicates that the deformation rate of POPC bilayers are not affected at a given shear rate and they exhibit Newtonian rheology.

Eq. 2 in the main text shows that the slope depends on t_{d}, which depends on the field amplitude E_0, and p^{el}, which depends on frequency. Hence to isolate the viscosity, one needs to plot the deformation data as a function of time rescaled as $t/t_{\mathrm{d}}p^{\mathrm{el}}$, see Figure Fig. S5.

C. Bending rigidity values from Flickering Spectroscopy and capacitance measurements for electrodeformation method

The method for flickering spectroscopy is detailed in [9, 10]. Here, we summarize the electrodeformation method to extract out membrane capacitance. The procedure follows the original approach developed by *Salipante et al.* [11]. The vesicle shape morphology with conductivity ratio $\Lambda > 1$ is always prolate. However, for $\Lambda < 1$, the conductivity of the outer solution is higher than the vesicle solution and the aspect ratio/deformation parameter $s(\omega)$ is positive at low frequencies that is prolate shape. As the frequency increases, the vesicles becomes less prolate and adopts a spherical shape at a certain frequency. Above this critical frequency, the vesicles adopt an oblate shape. The critical frequency can be approximated as:

$$\omega_c = \frac{\lambda_{\mathrm{in}}}{RC_{\mathrm{m}}} \frac{1}{\sqrt{(1-\Lambda)(3+\Lambda)}} \tag{10}$$

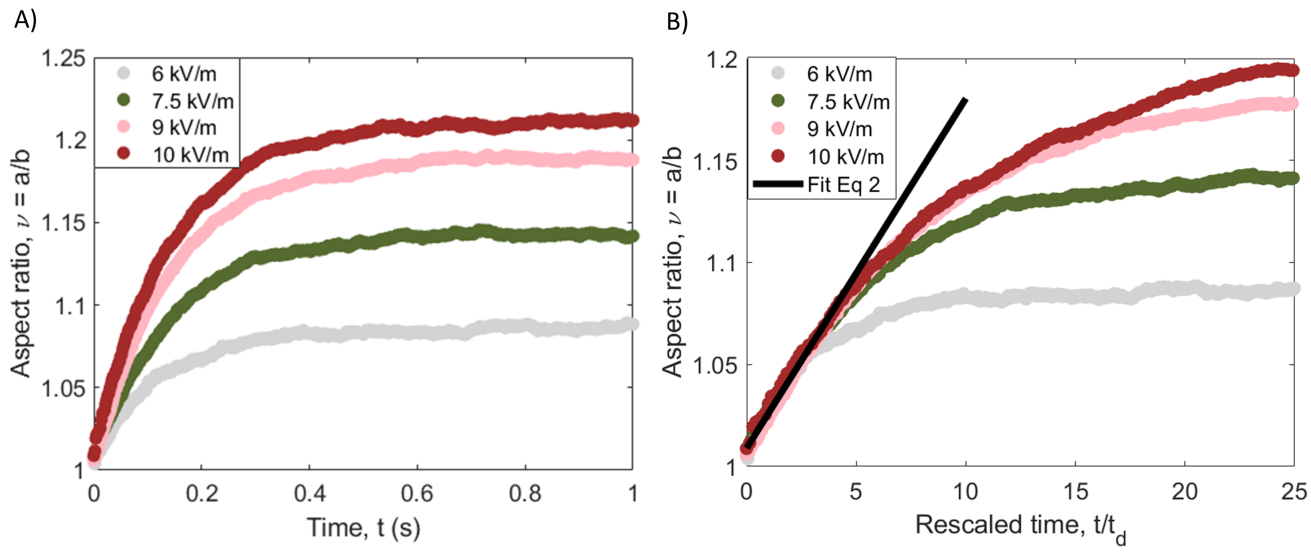

Fig. S 4: (A) Deformation curves for a POPC vesicle (R= 30.1 μm) exposed to fields of different amplitudes (at 1 kHz). (B) The initial slope of the data in (A) re-plotted as a function of the re-scaled time $t/t_{\rm d}$ yields an apparent membrane viscosity $\eta_m = 2.63 \pm 0.41 \times 10^{-7}$ Pa.s.m.

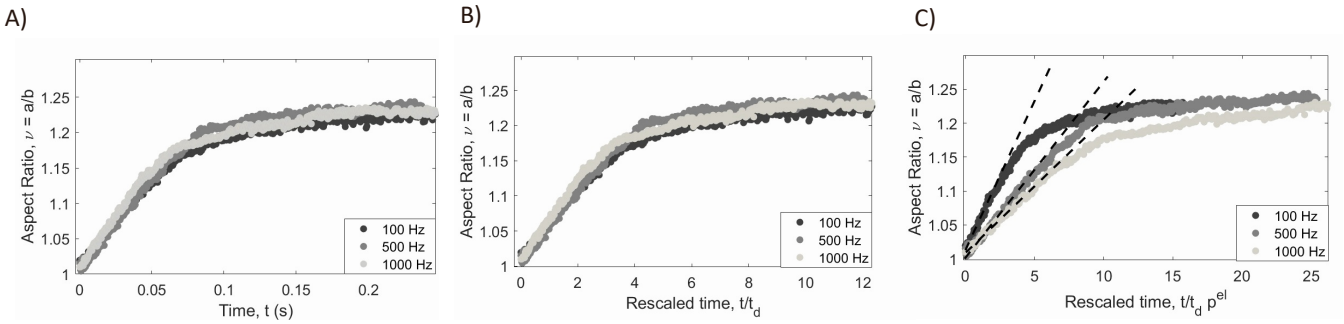

Fig. S 5: (A) Deformation curves for a POPC vesicle (R= 14.7 μm) exposed to fields of different frequency but same field amplitude $E_0 = 8$ kV/m. (B) The initial slope of the data in (A) re-plotted as a function of the re-scaled time $t/t_{\rm d}$, see Figure Fig. S5. The electric stress $p^{\rm el}$ increases with frequency but the slope in (B) remains the same indicating that apparent surface viscosity also increases. (C) Indeed, when data are plotted vs $t/t_{\rm d}p^{\rm el}$ the slope decreases with increasing frequency yielding the frequency dependence of the apparent viscosity. Extrapolation to zero frequency gives the membrane viscosity

Hence, the membrane capacitance can be determined from the experimentally measured critical frequency based on prolate-oblate transition with a frequency sweep [11]. The measured bending rigidity and capacitance values are summarized in Table I.

Table S I: Membrane bending rigidity and capacitance of phospholipids, polymers PBd_x-*b*-PEO_y and mixed system of DOPC:DPPC:Chol at 25 ^{o}C determined in this study. Bending rigidity was measured with flickering spectroscopy and membrane capacitance was measured with the electrodeformation method. M_w and M_h refer to the total and hydrophobic molecular weight, respectively. NA means not available.

Composition	M_w [kDa]	M_h [kDa]	κ ($k_B\,T$)	C_m ($\mu F/cm^2$)
POPC	0.760	0.448	27.8 ±2.3	0.72 ± 0.04
SOPC	0.787	0.476	30.1 ±3.1	0.71 ± 0.02
DOPC	0.786	0.474	22.2 ±2.0	0.72 ± 0.04
OMPC	0.732	0.420	27.1 ±2.6	0.71 ± 0.03
DOPC:Chol (1:1)	NA	NA	27.8 ±4.6	0.50 ± 0.09
DPPC:Chol (1:1)	NA	NA	121.3 ±11.0	0.45 ± 0.05
DOPC:DPPC:Chol (1:1:1)	NA	NA	72.0 ±8.4	0.51 ± 0.16
DOPC:DPPC:Chol (1:1:2)	NA	NA	69.2 ±7.9	0.63 ± 0.10
PBd_{13}-*b*-PEO_{11}	1.19	0.7	17.1 ±1.5	0.36 ± 0.05
PBd_{22}-*b*-PEO_{14}	1.80	1.35	31.0 ±5.1	0.27 ± 0.03
PBd_{33}-*b*-PEO_{20}	2.60	1.85	54.4 ±6.4	0.23 ± 0.04
PBd_{46}-*b*-PEO_{24}	3.54	2.60	NA	0.18 ± 0.03
PBd_{54}-*b*-PEO_{29}	4.19	3.10	154± 16.0	0.18 ± 0.04
PBd_{120}-*b*-PEO_{78}	9.91	6.80	NA	0.07 ± 0.01

Table S II: Membrane viscosities and values of a dye diffusion coefficient (DiC18) for the DOPC:DPPC:Chol ternary system. The values in brackets indicate lipid molar ratios (first column) and the number of measured vesicles (third column). All the experiments were performed at 25.0 ^{o}C. L_d and L_o denote liquid disordered and liquid ordered, respectively. The diffusion coefficient were taken from [12]

Multi-component	Phase state	η_m [nPa.s.m]	D [μm^2/s [12]]
DOPC	L_d	4.11 ±2.63 (20)	6.30±0.13
DPPC:Chol (1:1)	L_o	56.4 ±4.63 (25)	0.48±0.06
DOPC:DPPC:Chol (1:1:2)	L_o	15.4 ±2.40 (25)	1.85±0.13
DOPC:DPPC:Chol (1:1:1)	L_d	17.7 ±3.06 (18)	2.50±0.20
DOPC:Chol (1:1)	L_d	7.00 ±4.77 (25)	3.25±0.25

3. MOVIE DESCRIPTION

Videos showing the deformation and relaxation of GUVs made of POPC (left) and PBd_{33}-*b*-PEO_{20} (right) with radii of 31 and 24 μm, respectively. The videos were acquired with phase contrast microscopy at E_o= 10 kV/m at 1 kHz. The time stamps show the actual time.

[1] P. M. Vlahovska, R. S. Gracia, S. Aranda-Espinoza, and R. Dimova. Electrohydrodynamic model of vesicle deformation in alternating electric fields. Biophys. J., 96:4789–4803, 2009.

[2] P. M. Vlahovska. Non-equilibrium dynamics of lipid membranes: deformation and stability in electric fields. In A. Iglic, editor, Advances in Planar Lipid Bilayers and Liposomes, vol. 12, pages 103–146. Elsevier, 2010.

[3] Petia M. Vlahovska. Electrohydrodynamics of drops and vesicles. Annu. Rev. Fluid Mech., 51:305–330, 2019.

[4] Petia M. Vlahovska and C. Misbah. Theory of vesicle dynamics in flow and electric fields. In R. Dimova and C. Marques, editors, The Giant Vesicle Book, page Chapter 7. CRC Press, 2019.

[5] E. Evans and W. Rawicz. Entropy driven tension and bending elasticity in condensed-fluid membranes. Phys. Rev. Lett., 64:2094–2097, 1990.

[6] U. Seifert. Fluid membranes in hydrodynamic flow fields: Formalism and an application to fluctuating quasispherical vesicles. Eur. Phys. J. B, 8:405–415, 1999.

[7] D. Needham and R. M. Hochmuth. Electromechanical permeabilization of lipid vesicles. role of membrane tension and compressibility. Biophys. J., 55:1001–1009, 1989.

[8] Rumiana Dimova, Natalya Bezlyepkina, Marie Domange Jordö, Roland L. Knorr, Karin A. Riske, Margarita Staykova, Petia M. Vlahovska, Tetsuya Yamamoto, Peng Yang, and Reinhard Lipowsky. Vesicles in electric fields: Some novel aspects of membrane behavior. Soft Matter, 5:3201–3212, 2009. doi:10.1039/B901963D. URL `http://dx.doi.org/10.1039/B901963D`.

[9] Hammad A. Faizi, Shelli L. Frey, Jan Steinkühler, Rumiana Dimova, and Petia M. Vlahovska. Bending rigidity of charged lipid bilayer membranes. Soft Matter, 15(29):6006–6013, 2019. ISSN 1744-683X. doi:10.1039/C9SM00772E. URL `http://dx.doi.org/10.1039/C9SM00772E`.

[10] Hammad A. Faizi, Cody J. Reeves, Vasil N. Georgiev, Petia M. Vlahovska, and Rumiana Dimova. Fluctuation spectroscopy of giant unilamellar vesicles using confocal and phase contrast microscopy. Soft Matter, 16:8996–9001, 2020. doi:10.1039/D0SM00943A. URL `http://dx.doi.org/10.1039/D0SM00943A`.

[11] P. F. Salipante, R. Knorr, R. Dimova, and P. M. Vlahovska. Electrodeformation method for measuring the capacitance of bilayer membranes. Soft Matter, 8:3810– 3816, 2012.

[12] Dag Scherfeld, Nicoletta Kahya, and Petra Schwille. Lipid dynamics and domain formation in model membranes composed of ternary mixtures of unsaturated and saturated phosphatidylcholines and cholesterol. Biophysical Journal, 85(6):3758 – 3768, 2003. ISSN 0006-3495. doi:https://doi.org/10.1016/S0006-3495(03)74791-2. URL `http://www.sciencedirect.com/science/article/pii/S0006349503747912`.